

# **A Finite Element Analysis of Laser Transmission Welding of Polycarbonate**

Moussa Magara Traoré, Sekou Singare

ECOLE NORMALE D'ENSEIGNEMENT TECHNIQUE ET PROFESSIONNEL, MALI

**ABSTRACT:** The influence of process parameters on temperature distribution during laser transmission welding of polycarbonate is investigated in the present research work. A transient numerical, based on conduction mode heat transfer, is developed to analyze the process. Temperature field was obtained by a numerical solution the transient heat transfer equation with activity of inner heat sources using finite element method. Temperature distribution analysis in welded joint was performed in the ABAQUS/Standard solver. Power distribution of moving heat source was implemented into DFLUX subroutine, written in FORTRAN programming language. The heat input to the model is assumed to be a volumetric Gaussian heat source. Temperature dependent physical properties of the materials are taken into account during modeling. Combined heat transfer boundary condition, based on natural convection and radiation, is imposed on model exteriors, which are exposed to surroundings. Temperature distribution in the weld zone was numerically estimated. The weld strength and microstructure of the lap weld were determined experimentally and validate by finite element analysis result.

**KEYWORDS:** Laser transmission welding, finite element modeling, process parameters, polycarbonate

## **I. INTRODUCTION**

The main goal of welding is to achieve a strong joint between two parts. Ideally, the strength of a weld line should be close to the strength of the joined materials. Therefore, the influence of different parameters on the weld strength was extensively studied.

Mian and Mahmood<sup>[1]</sup> modeled a three-dimensional uncoupled finite element analysis for glass and polyimide. Acherjee et al.<sup>[2]</sup> presented a transient simulated model to analyze the LTW process. It turned out that the carbon black had a considerable influence on the temperature field and weld pool geometry. Becker et al.<sup>[3]</sup> presented a two-dimensional thermal model to simulate the heating phase of the LTW and the simulation results showed a good agreement with the experimental values. Mahmood et al.<sup>[4]</sup> set a three-dimensional heat transfer model to determine the optimum process parameters of jointing polyimide and titanium. It was found that with a power of 4.0 W, good bonding could be formed when the scanning speed was between 600 and 2000 mm/min. Mayboudi and Birk<sup>[5]</sup> developed a two-dimensional thermal finite element model of the LTW for T-joint. The 2D model was used to predict the transient temperature distribution along the welding path as well as the depth of the molten zone. Zoubeir and Elhem<sup>[6]</sup> developed a finite element model to predict the temperature field and the residual distribution after the LTW process of a mini-tank. The results showed that both the temperature generated and the clamping pressure greatly influenced the bending phenomena during the LTW process. A three-dimensional transient thermal model of LTW was developed by Van de Ven et al.<sup>[7]</sup> to investigate the LTW process of polyvinyl chloride and the error between the model and experimental values was 4.3%.

Numerical analysis of the temperature field in elements heated by a movable heat source was performed in ABAQUS/Standard module. Power distribution of moving heat source was implemented into DFLUX subroutine, written in FORTRAN programming language. Temperature-dependent thermophysical properties were taken into account in the numerical model<sup>[10]</sup>. Gaussian laser beam is used in calculations in order to analyze the influence of process parameters such as welding speed on the welded zone.

# International Journal of Innovative Research in Science, Engineering and Technology

(A High Impact Factor, Monthly, Peer Reviewed Journal)

Visit: [www.ijirset.com](http://www.ijirset.com)

Vol. 7, Issue 12, December 2018

## II. FINITE ELEMENT SIMULATION OF LASER TRANSMISSION WELDING

### 2.1 Thermal model formulation

The transient temperature field generated during the laser welding is determined based on the mechanism of heat conduction:

$$\rho \cdot c \frac{\partial T}{\partial t} = \nabla \cdot (k \nabla T) + q_v \quad (1)$$

Where,  $\rho$  is material density,  $c$  is the specific heat,  $T$  is the temperature,  $t$  is the time,  $k$  is the thermal conductivity,  $\nabla$  is the gradient operator and  $q_v$  is the rate of internal heat generation per unit volume and is given by:

$$q_v(x, y, z, t) = \begin{cases} 0 & ; \text{for transparent part} \\ (1-R_a)KI_a e^{-kz} & ; \text{for absorbing part} \end{cases} \quad (2)$$

where,  $R_a$  is the reflectivity of the absorbing material,  $K$  is the absorption coefficient of the absorbing material,  $z_a$  is the depth within the absorbing materials, and  $I_a$  is the laser intensity (having Gaussian distribution) after passing through the transparent material, which can be further expressed as:

$$I_a = \frac{T_t P}{\pi r_0^2} \exp\left(-\frac{r^2}{r_0^2}\right) \quad (3)$$

where  $T_t$  is the transmission factor of transparent polymer part,  $P$  is the laser power (W),  $r_0$  is the laser beam radius (radius of Gauss function curve), and  $r$  is the radial distance of any point on the surface of the material;  $r = \sqrt{x_s^2 + y_s^2}$ ,

where  $x_s$  and  $y_s$  are the Cartesian coordinates of that point. The laser system considered for this study is a continuous wave diode laser system having an operational wave length of 1064nm. The transmission factor of a 4 mm thick transparent PC plaque at 1064nm laser radiation is 0.90, as measured using a laser power meter.

At the initial condition when time=0s, the workpieces are at uniform ambient temperature. The environmental temperature is chosen as  $T_0=27^\circ\text{C}$ .

For the heat transfer between the workpieces and the surrounding medium the boundary condition can be written as:

$$-k(T)\nabla T \cdot \vec{n} = h(T_s - T_0) + \varepsilon\sigma(T_s^4 - T_0^4) \quad (4)$$

where,  $\vec{n}$  is the normal vector of the surface,  $h$  is the convection heat transfer coefficient,  $T_s$  is the surface temperature,  $T_0$  is ambient temperature,  $\varepsilon$  is the material emissivity,  $\sigma$  is the Stefan Boltzmann constant. Convective heat transfer coefficient,  $h$ , is assumed to be  $5 \text{ W/m}^2\text{K}$  [8].

### 2.2 Finite element simulation

A 3D finite element method thermal model of a lap-joint geometry exposed to moving laser was developed using ABAQUS software. The materials considered are natural and opaque polycarbonates. The transparent part transmission is 0.90, and absorbing part absorption coefficient of polycarbonate is determined using the relationship:  $y=82x$ , where  $y$  is the absorption coefficient ( $\text{mm}^{-1}$ ) of the polycarbonate containing  $x$  percent carbon black by weight [9] (fig.1).

Temperature dependent physical properties (thermal conductivity, specific heat, and density) of the materials are used for thermal modeling [10], which is furnished in Table 1.

Gaussian heat flux is applied on the material body on which the laser is being focused. The heat flux is calculated as a function of beam dimensions, laser power and absorption coefficient of the absorbent parts using Equation (2). A look-up table is made to create the heat generation input file in the form of a 3-D array and is a function of  $x$ ,  $y$  and  $z$  coordinates. The moving load is applied by a subroutine implemented in FORTRAN programming language. The load moves with time. Thus, a nodal temperature history is obtained as a function of time. The time is calculated based on the welding speed and heat source location. The transient heat transfer mode is then run and nodal temperature is documented as a function of time for use in the subsequent steps.

# International Journal of Innovative Research in Science, Engineering and Technology

(A High Impact Factor, Monthly, Peer Reviewed Journal)

Visit: [www.ijirset.com](http://www.ijirset.com)

Vol. 7, Issue 12, December 2018

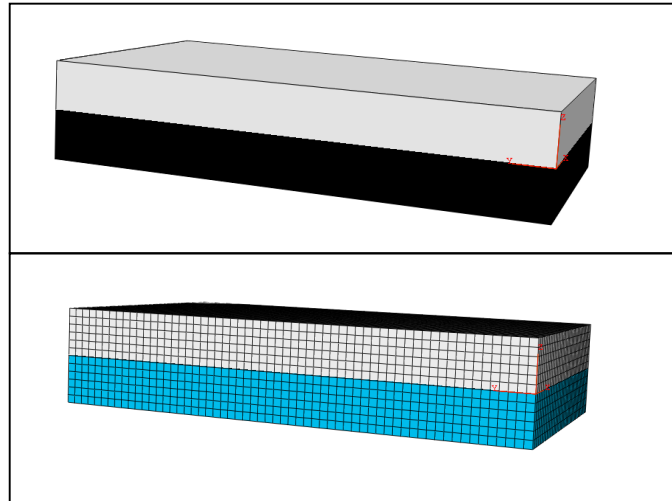


Fig. 1 Schematic of the sample and 3D meshed model for the lap-joint configuration

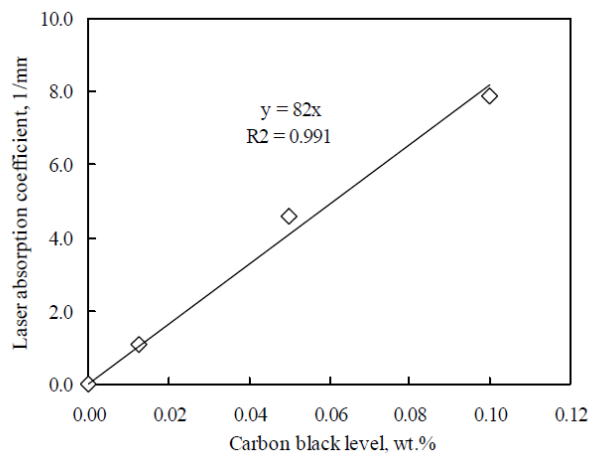


Figure 2 Laser absorption coefficients as a function of carbon black level for PC<sup>[9]</sup>

Table 1 Temperature dependent physical properties of polycarbonate used for numerical simulation<sup>[10]</sup>.

Properties	Temperature dependent data
Density, $\rho$ (kg/m <sup>3</sup> )	$\rho = -0.319T + 1207$ , for $27^\circ\text{C} \leq T \leq 145^\circ\text{C}$ $\rho = -0.685T + 1253$ , for $T > 145^\circ\text{C}$
Thermal conductivity, $k$ (W/m K)	$k = (2.493 \text{ E-}4) T + 0.186$ , for $27^\circ\text{C} \leq T \leq 145^\circ\text{C}$ $k = (-5.536 \text{ E-}5) T + 0.230$ , for $T > 145^\circ\text{C}$
Specific heat, $C$ (J/kg K)	$C = 3.420 T + 1120.67$ , for $27^\circ\text{C} \leq T \leq 140^\circ\text{C}$ $C = 27.385 T - 2236.38$ , for $140^\circ\text{C} \leq T < 147^\circ\text{C}$ $C = 1.771 T + 1537.41$ , for $T \geq 148^\circ\text{C}$

## International Journal of Innovative Research in Science, Engineering and Technology

(A High Impact Factor, Monthly, Peer Reviewed Journal)

Visit: [www.ijirset.com](http://www.ijirset.com)

Vol. 7, Issue 12, December 2018

### Results of temperature field simulation

In this simulation, the PC transparent part and absorbing part are welded by using a laser power of 40 W, a welding speed of 40 mm/s. Fig. 3 shows the temperature distributions on the lapped (X–Y) plane with a moving heat source at four selected time points: (a)  $t = 0.15$  s when the laser beam just contacts the lapped parts to be welded, (b)  $t = 15$  s when the laser beam is just arriving at the center of the parts, (c)  $t = 32$  s when the laser beam is at the end of the parts and (d)  $t = 34$  s when the welding parts have been cooled for 2 s. It can be seen from this figure that the maximum temperature of 333.8 °C is achieved during the welding, which is greater than the glass transition temperature (150 °C) of polycarbonates. The weld width can be determined at the weld interface where the temperature is more than 150 °C. The region in the contours plot temperature above 150 °C, shows the molten depth in both the polycarbonate parts from weld interface.

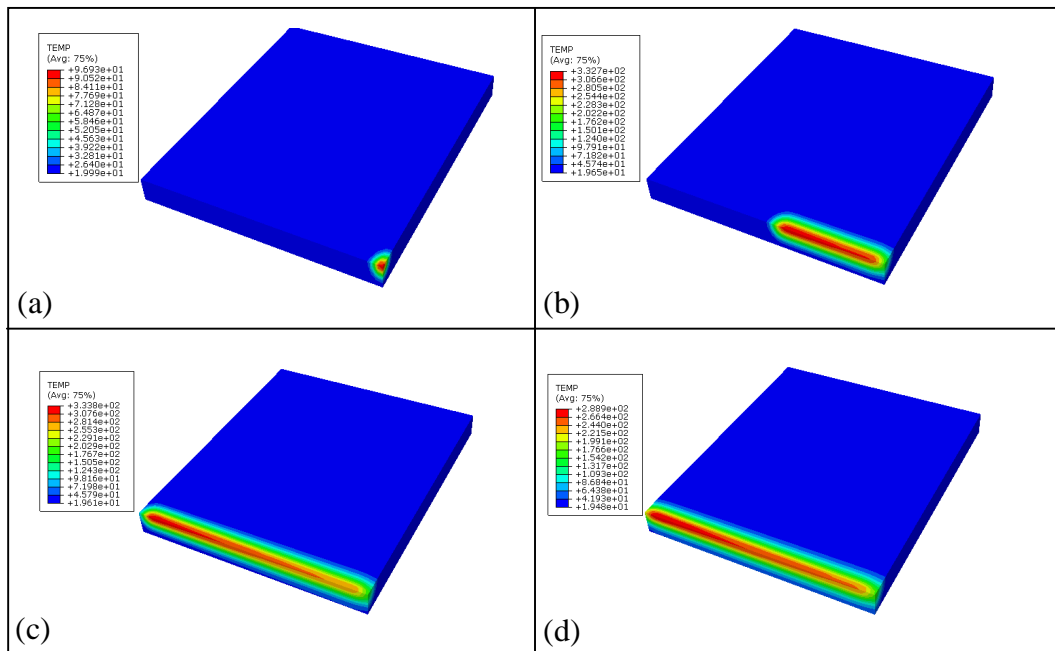


Figure 3: Temperature distributions on the lapped (X–Y) plane: (a)  $t = 0.15$  s, (b)  $t = 15$  s, (c)  $t = 32$  s and (d)  $t = 34$  s.

The influence of welding speed on the temperature field is studied using the finite element model. Figure 4 the temperature distribution on the lapped (X–Y) plane at different welding speed. At welding speed of 10 mm/s a maximum welding temperature reach 589.5 °C (fig.4 (a)), however, the polycarbonate starts decomposing at 500 °C. The temperature above this range can cause partial degradation of the materials. As the welding speed increase to 100 mm/s, the temperature decrease to 165.5 °C which is slightly higher than the glass transition temperature of Polycarbonate (150 °C). The bond starts to form at the weld interface when the temperature reaches 150 °C.

# International Journal of Innovative Research in Science, Engineering and Technology

(A High Impact Factor, Monthly, Peer Reviewed Journal)

Visit: [www.ijirset.com](http://www.ijirset.com)

Vol. 7, Issue 12, December 2018

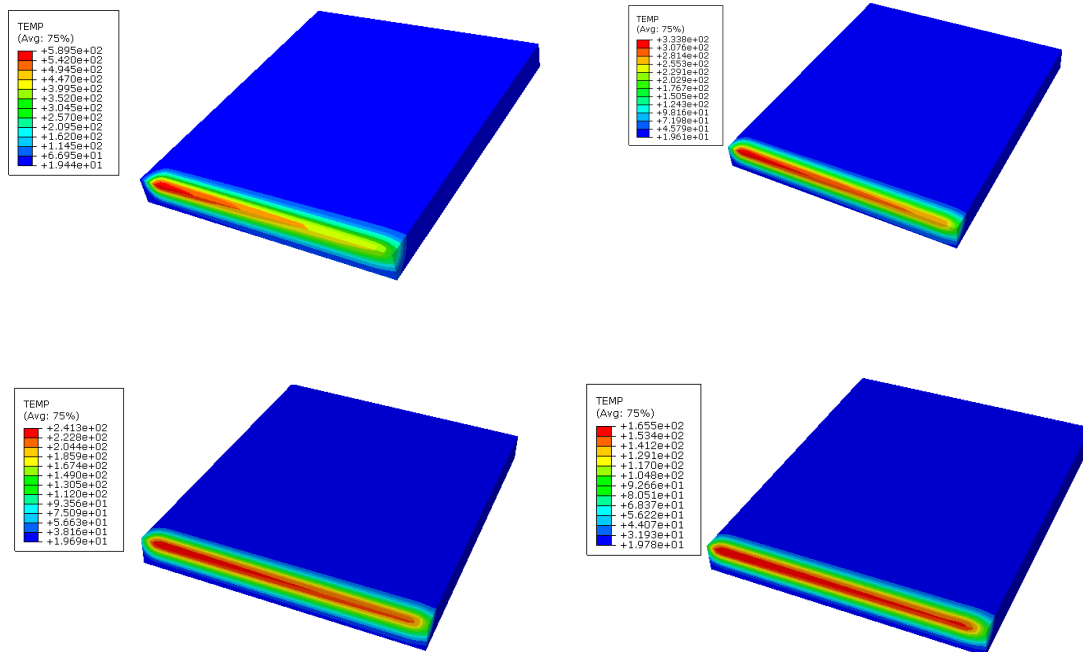


Figure 4 Temperature distributions on the lapped (X–Y) plane: (a) welding speed  $v = 10$  mm/ s, (b)  $v = 40$  mm/ s, (c)  $v = 80$  mm/s and (d)  $v = 100$  mm/ s.

## 2.3 Experimental equipments and preparatory work

The welding experiment were carried out using 200W Nd:YAG laser operating at 1064nm wavelength equipped with a 3-axes CNC work table, coordinated with the motion system and computer interface. A lap joint configuration was considered in the experiments, the laser-transparent part and the laser-absorbent part are welded together with a fixed overlap distance. The laser beam scans over the assembly at the specified power and speed to join the two parts together. The effects of welding speed on weld strength and microstructure were assessed. A shear lap tensile test with the weld line arranged perpendicular to the test pull direction was used to evaluate the weld quality of specimens.

## Results of validation

Fig.5 shows the force at break as a function of welding speed, at laser power of 40W. Welds formed at low welding speed, such as 10 mm/ s, resulting in low tensile strength 0.4KN, the maximum welding temperature reach 589.5 °C. The micrograph of the weld zone shows decomposition at this welding speed setting (fig.6 (a)). An increase of the welding speed to 40 mm/s resulted in increase of the weld strength. The maximum tensile strength of the joints is 1.3KN which is achieved at 40 mm/s of welding speed. In this welding speed range the maximum welding temperature of 333.8 °C is achieved during the welding, the weld width is wide and no welding defect is obtained during welding. Above 40 mm/s of welding speed, tensile strength, weld temperature are lower. The micrograph of the weld zone shows thin weld at high welding speed setting. On the other hand, the molten pool experienced lower temperature during welding. It undergoes maximum temperature slightly higher than the fusion temperature range of PC material. Therefore, the temperature gradient decreasing Along the vertical direction from the top surface toward the bottom surface, which result in low melting depth, as consequence lead to lower weld strength. In figure (6) the results indicate that the welding speed is the most important factor affecting the welded zone width. An increase in welding speed leads to a decrease in welded zone width. This is due to the laser beam travelling at high speed over the welding line when

## International Journal of Innovative Research in Science, Engineering and Technology

(A High Impact Factor, Monthly, Peer Reviewed Journal)

Visit: [www.ijirset.com](http://www.ijirset.com)

Vol. 7, Issue 12, December 2018

welding speed is increased. Therefore the heat input decreases leading to less volume of the material being melted, consequently the width of the welded zone decreases.

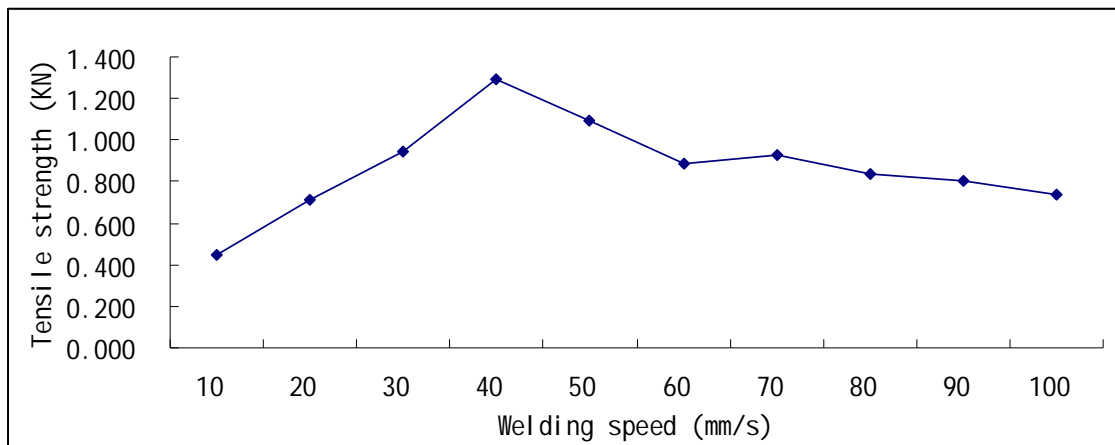


Figure 5: The tensile load as a function of welding speed, laser power=40W

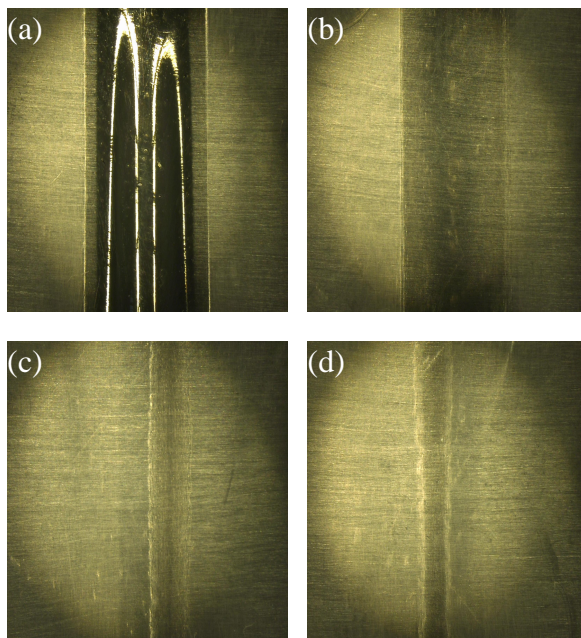


Figure 6: Effect of welding speed on weld microstructure, laser power 40W, transparent part thickness 3mm;  
(a)10mm/s; (b) 40mm/s; (c) 60mm/s; (d) 100mm/s.

### III. CONCLUSION

A finite element model has been developed based on the commercially available software, ABAQUS to determine the temperature distribution inside the polymer during laser welding. The numerically computed results are compared with the experimental results.

# International Journal of Innovative Research in Science, Engineering and Technology

(A High Impact Factor, Monthly, Peer Reviewed Journal)

Visit: [www.ijirset.com](http://www.ijirset.com)

Vol. 7, Issue 12, December 2018

The weld strength mainly depends on the welding defects and temperature distributions at the welded zone, of which are functions of the welding parameters. The lower tensile strength of joints is attributed to the lower temperature on the welded zone which should have affected the melt volume in this area especially at higher welding speed, therefore the heat input decreases leading to less volume of the material being melted.

## ACKNOWLEDGEMENT

This project is supported by Science and Technological Program for Dongguan's Higher Education, Science and Research, and Health Care Institutions (**Project No. 2011108101002**, and **Project No. 2012108101001**), Cooperation Project of Industry, Education and Academy of Guangdong Province, Guangdong Province Science and Technology Department (**Project No.2012B091000012**).

## REFERENCES

- [1] Ahsan M, Tonfiz M, Greg A, Reiner W, Hans H, Golam N. Effects of laser parameters on the mechanical response of laser irradiated micro-joints. *J Mater Res Soc* 2006;926
- [2] Bappa A, Arunanshu SK, Souren M, Dipten M. Effect of carbon black on temperature field and weld profile during laser transmission welding of polymers: A FEM study. *J Opt Laser Technol* 2012;44:514–21.
- [3] Becker F, Potente H. A step towards understanding the heating phase of laser transmission welding in polymers. *Polym Eng and Sci* 2002;42:365–74.
- [4] Mahmood T, Mian A, Amin MR, Auner G, Witte R, Herfurth H, et al. Finite element modeling of transmission laser micro joining process. *J Mater Process Technol* 2007;186:37–44.
- [5] Mayboudi LS, Birk AM, Zak G, Bates PJ. A two-dimensional thermal finite element model of laser transmission welding for T joint. *J Laser Appl* 2006;18:192–8.
- [6] Tourki Z, Ghorbel E. Numerical study of laser diode transmission welding of a polypropylene mini-tank: temperature field and residual stresses distribution. *Polym Testing* 2011;30:23–34.
- [7] Van de Ven JD, Erdman AG. Laser transmission welding of thermoplastics—Part I: Temperature and pressure modeling. *J Manuf Sci Eng* 2007;129:849–58.
- [8] Mayboudi L.S. A 2-D thermal model for laser transmission welding of thermoplastics. *Proceedings of the 24th International Congress on Applications of Lasers & Electro-Optics, 2005.* (Mayboudi, L.S., A.M. Birk, G. Zak, P.J. Bates)
- [9] M. Chen, G. Zak, P.J. Bates, *Laser absorption coefficient measurement of amorphous polymers for laser transmission welding*, ANTEC 2006, pp2291-2295
- [10] Acherjee B, Kuar AS, Mitra S, Misra D. Effect of carbon black on temperature field and weld profile during laser transmission welding of polymers: a FEM study. *Optics and Laser Technology* 2012;44(3):514–21.